SANDIA REPORT

SAND2003-8651
Unlimited Release
Printed December 2003

A Molecular- and Nano- Electronics Test (MONET) Platform Fabricated Using Extreme Ultraviolet Lithography

A. A. Talin, L. Hunter, G. F. Cardinale, and P. Dentinger

Prepared by
Sandia National Laboratories
Albuquerque, New Mexico 87185 and Livermore, California 94550

Sandia is a multiprogram laboratory operated by Sandia Corporation,
a Lockheed Martin Company, for the United States Department of Energy's
National Nuclear Security Administration under Contract DE-AC04-94AL85000.

Sandia National Laboratories

Issued by Sandia National Laboratories, operated for the United States Department of Energy by Sandia Corporation.

Available to DOE and DOE contractors from
U.S. Department of Energy
Office of Scientific and Technical Information
P.O. Box 62
Oak Ridge, TN 37831

Telephone: (865)576-8401
Facsimile: (865)576-5728
E-Mail: reports@adonis.osti.gov
Online ordering: http://www.doe.gov/bridge

Available to the public from
U.S. Department of Commerce
National Technical Information Service
5285 Port Royal Rd
Springfield, VA 22161

Telephone: (800)553-6847
Facsimile: (703)605-6900
E-Mail: orders@ntis.fedworld.gov
Online order: http://www.ntis.gov/help/ordermethods.asp?loc=7-4-0#online

SAND2003-8651
Unlimited Release
Printed December 2003

A Molecular- and Nano- Electronics Test (MONET) Platform Fabricated Using Extreme Lithography

A. A. Talin and L. Hunter
Nanolithography Department 8751
G. F. Cardinale
Microsystems Design and Integration Department 8245
P. Dentinger
Material Chemistry Department 8762
Sandia National Laboratories, Livermore, CA 94550

Abstract

We describe the fabrication and characterization of an electrode array test structure, designed for electrical probing of molecules and nanocrystals. We use Extreme Ultraviolet Lithography (EUVL) to define the electrical test platform features. As fabricated, the platform includes nominal electrode gaps of 0 nm, 40 nm, 60 nm, and 80 nm. Additional variation in electrode gap is achieved by controlling the exposure conditions, such as dose and focus. To enable EUVL based nanofabrication, we develop a novel bilevel photoresist process. The bilevel photoresist consists of a combination of a commercially available polydimethylglutarimide (PMGI) bottom layer and an experimental EUVL photoresist top (imaging) layer. We measure the sensitivity of PMGI to EUV exposure dose as a function of photoresist pre-bake temperature, and using this data, optimize a metal lift-off process. Reliable fabrication of 700 Å thick Au structures with sub-1000 Å critical dimensions is achieved, even without the use of a Au adhesion layer, such as Ti. Several test platforms are used to characterize electrical properties of organic molecules deposited as self assembled monolayers.

Acknowledgement

The authors would like to thank the 10x Microstepper tool team D. Folk, J. Selfridge, K. McDonald, C. Steinhous for their participation in fabricating the structures described here, and to John Goldsmith and Bill Ballard for useful discussions and support.

Table of Contents

A Molecular- and Nano- Electronics Test (MONET) Platform Fabricated Using Extreme Ultraviolet Lithography

1. Introduction

The motivation for creating a Molecular and Nano- Electronics Test platform (MONET) arises from two principal factors. First, molecular switches are seen by many leading technologists in industry and academia as the eventual replacement for the traditional Si based transistors in integrated circuits [1-4]. The second reason is the possibility of creating new biological sensors: for example, several groups have reported sequence dependent charge transport in DNA [5,6].

However, despite significant progress and increasing interest in molecular electronics, basic results on electrical transport in molecules have been difficult to reproduce from lab to lab, and many promising compounds have yet to be tested. This is partly due to the long lead times and high expense associated with the fabrication of test structures, which inevitably require electron beam lithography. Thus, experiments designed to test important variables such as the electrode metal, contact chemistry, molecular deposition method, in addition to the actual molecule being investigated, become impractical for most researchers. Here we describe the use of EUVL for fabrication of such a platform and report preliminary results on application of this platform for characterization of several different types of organic molecules.

2. EUVL Based Nanofabrication

EUVL is a leading candidate technology to meet the future lithography requirements for semiconductor manufacturing, and substantial progress has been made in transferring this technology from research laboratories into production [7]. Nevertheless, very little actual device fabrication using EUVL has occurred since the technique was invented over a decade ago [8]. One of the challenges of EUVL-based manufacturing is that the typical EUVL photoresist thickness is on the order of 1000 Å. However, for most etch-based pattern-transfer processes, a thicker photoresist layer is preferable, since this lowers the bias requirement between the material being etched and the photoresist [9]. Lift-off is another common fabrication process for which a thicker photoresist layer is desirable [10]. A common approach to increase the effective photoresist thickness is to use a bilayer photoresist stack. The important requirements for successful implementation of a bilevel photoresist stack are that the layers do not intermix, and that the effects of the top layer deposition and exposure on the subsequent performance of the

under-layer are known [10]. In this work we used a bilevel photoresist combination consisting of polydimethylglutarimide (PMGI) as the under-layer and our baseline EUV positive-tone photoresist, Shipley EUV-2D (S2D) as the top imaging layer. PMGI is a well-known lift-off photoresist, since it is compatible with a wide range of positive photoresists, it is not sensitive to I-line radiation, and its dissolution rate in tetramethyl ammonium hydroxide (TMAH) can be adjusted by controlling the PMGI pre-bake temperature [11,12]. We develop the bilevel photoresist primarily to facilitate EUVL based nanofabrication of a molecular electronics test platform using metal lift-off.

3. Effect of EUV Exposure on PMGI Dissolution Rate in TMAH

PMGI was supplied by Microchem Corp., and all experiments reported in this paper were carried out using the PMGI 'Slow' formulation [12]. Since the dissolution rate of PMGI in TMAH is highly dependent on the pre-bake temperature, we chose three prebake temperatures for which to determine the EUVL sensitivity: 200°C, 250°C, and 300°C. All substrates used were 4" Si(100) wafers. Prior to spin-coating PMGI, the Si wafers were heated on a hot-plate for five minutes at 200°C (250°C, 300°C) to remove excess moisture. After allowing the substrate to cool, PMGI was spin-coated at a speed of 1500 rpm for 30 sec, and immediately placed on the hot-plate for a five minute pre-bake at 200°C (250°C, 300°C). Prior to EUV exposures, the PMGI film thickness was measured using a Nanospec 2000AFT reflectometer. EUV exposures were carried out using the Sandia 10× Microstepper tool [13]. For a given wafer, 10 separate fields were printed, each corresponding to a different EUV dose, ranging from 1.67 mJ/cmP^{2P} to 5.86 mJ/cmP^{2P}. Exposed PMGI wafers were developed in 0.26 N TMAH. To accurately establish the dissolution rate, three wafers were processed for a given prebake temperature, and developed for 15 sec, 30 sec, and 45 sec. The removed thickness of PMGI was again measured, and the rate calculated based on the average value for the three development times. The dissolution rate of PMGI versus EUV exposure dose for three pre-bake temperatures is shown in Figure 1. As expected the dissolution rate decreases with increasing pre-bake temperature. For all three temperature, the rate increases linearly up to a dose of 3 mJ/cmP^{2P}, beyond which value the rate levels off to ~60 Å/sec.

For the fabrication of bilevel photoresist stacks we used S2D photoresist as the top imaging layer. This photoresist has been studied extensively for EUVL application and its characteristics are well known [14]. Based on the results shown in Figure 1, we chose two PMGI prebake temperatures for the bilevel experiments: 200°C, and 250°C. Following the deposition of PMGI, S2D photoresist was spin coated to a nominal thickness of 1250 Å, after which the wafer was baked at 130°C for 60 sec, exposed, and baked again at 130°C for 90 sec. Both wafers were developed in 0.26 N TMAH for 60 sec, and the remaining PMGI was measured using the Nanospec reflectometer. These results are summarized in Figure 2. While the bilevel stack with 200°C annealed PMGI layer completely cleared with EUV dose of 3 mJ/cmP^{2P}, the stack with the 250°C PMGI was not be completely cleared even for the highest dose used of 9 mJ/cmP^{2P}. These results were confirmed by cross-section images of the samples, collected using a Hitachi 4500 field emission scanning electron microscope (SEM), and shown in Figure 3 (a) and 3 (b) for the 200°C and 250°C samples, respectively. In addition to the nominal PMGI thickness of 1000 Å, we also prepared bilevel photoresists consisting of 300 Å PMGI/ 1250 Å S2D. The

thinner PMGI layer was completely cleared at a dose of 3 mJ/cmP^{2P} with only 45 sec of develop time in TMAH. SEM images corresponding the thinner PMGI/S2D combination are shown in Figure 3(c).

4. Metal Lift-Off Results

To evaluate the effectiveness of the bilevel photoresist stack for metal lift-off, several Si and Si/$SiOB_{2B}$ substrates were coated with PMGI/S2D layers, exposed, developed, coated with Au metal using a CHA electron beam evaporator, and soaked in acetone. The results were compared to wafers coated with only S2D. In all cases, the nominal S2D thickness was 1250 Å. In figure 4 (a) we show SEM image of a Au pattern obtained following lift-off using only a single layer S2D photoresist. The image in 4 (a) clearly shows that the some of the Au features are peeling off the surface. In figure 4 (b) a similar Au pattern is shown for a wafer processed with the bilevel photoresist stack of 300 Å PMGI/1250 Å S2D prebaked at 250°C. Both wafers shown in figure 4 were coated simultaneously with 600 Å of Au, without any adhesion promoting metal layers, such as Cr or Ti. Generally, we found that for Au thickness of 700 Å and less, 300 Å of PMGI was sufficient to yield clean lift-off. For thicker Au layers, PMGI thickness of 1000 Å was required.

5. Molecular and Nanocrystal Electronic Test Platform Fabrication and Characterization

Recently, several groups have shown that single nanoparticles and nanotubes can be trapped between two electrodes using dielectrophoresis [15-17]. Furthermore, molecules of interest assembled on the electrodes can be bridged using dielectrophoretically trapped conducting nanoparticles, and electrically interrogated [17]. Following this approach, we fabricated a Mo/Si multilayer EUVL mask with TiN absorber layer for the 10× Microstepper which consists of an array of electrodes with nominal gaps of 0 nm, 400 nm, 500 nm, 600 nm, 700 nm, and 800 nm. A SEM image of the mask is shown in Figure 5 (a). In Figure 5 (b) we provide an optical image with SEM insets of a completed Au electrode structure fabricated using the mask shown in 5 (a) and the lift-off process described in preceding sections with 300 Å PMGI/1250 Å S2D photoresist. Electron beam lithography was not used in any phase of fabrication of this structure.

Since EUVL is a purely optical technique, it offers the benefit that dose and focus can be easily adjusted from field to field. Adjusting these parameters provides additional control over the final gap dimensions. As an example, we show in figure 6 the as-fabricated gaps corresponding to a nominal '0 nm' gap on the mask, and all printed on the same Si/$SiOB_{2B}$ wafer, patterned using EUV dose settings of 3.23 mJ/cmP^{2P}, 3.71 mJ/cmP^{2P} and 4.26 mJ/cmP^{2P}, 300 Å/1250 Å PMGI/S2D photoresist and 600 Å of Au.

6. Electrical Transport Using Bridged Au Nanospheres

In order to fully characterize the MONET platform we begin with electrical transport properties of nominally clean Au electrodes bridged with Au nanospheres. Au nanospheres of 30 nm, 60 nm, and 100 nm suspended in aqueous solutions were obtained commercially and used 'as-received'. A drop of ~30 □L of nanosphere solution was deposited on top of electrode structures and a bias of 1 V - 4 V peak-to-peak (pp) was applied across the electrodes. The frequency of the signal was varied from 10 kHz to 5 MHz. The ac voltage was applied for periods of 20 sec to 5 min. Typically, 20 sec is sufficient to deposit several nanospheres across the electrodes. A 1 M□ ballast resistor was used to limit current across particles once deposition occurred. Following deposition, the electrodes were rinsed in isopropanol and dried with nitrogen. An electrical probe station with a computer controlled Keithley 6487 picoammeter/voltage source was used for electrical testing. An SEM image of a string of 100 nm spheres bridging two electrodes is shown in figure 7 (a), and a current-voltage (I/V) plot corresponding to this junction is shown in figure 7 (b). The very high resistance and non-linear I/V profile are typical for nanosphere bridged junctions with as-fabricated Au electrodes. In addition to non-linear I/V characteristics, abrupt jumps in current were also observed as can be seen in figure 8. The typical resistance range for nanosphere bridged junctions on as-fabricated Au electrodes is 0.1 GΩ to 10 GΩ. Considerably lower, ohmic resistance on the order of 100 Ω was only recorded for 30 nm nanosphere junctions for which considerable melting of the particles as also observed, as shown in figure 9.

To find an explanation for such high resistance and non-linearity in I/V profiles, we analyzed the surface composition of as-fabricated Au electrodes using Auger electron spectroscopy (AES). A typical spectrum is shown in figure 10 (a), where it can be seen that a large amount of carbon is present on top of the electrodes. No carbon was observed on top of SiO_2 regions. Following this discovery, all subsequent MONET platforms are subjected to a gentle O_2 plasma etch at 60 Watts, 0.75 Torr for 3 min. This plasma treatment removes most of the carbon, as can be seen in figure 10 (b), with a small amount likely due to exposure of sample to lab air after cleaning. Nanosphere junctions formed following the cleaning procedure show lower resistance and ohmic (i.e. linear) I/V profiles, as can be seen in figure 11.

Once typical I/V characteristics for nominally clean Au electrodes have been established, bridged junctions with coated electrodes were investigated. Three different molecular species were investigated: $C_{14}H_{29}$-SH, C_6H_{11}-SH, and HS-C_6H_4-SH. The first two molecular species are considered insulators, with expected current of ~10^{-20} Amps /molecule [18], while the last molecule, benzene dithiol, is a conductor, with a previously measured current of ~10^{-8} Amps/molecule. The molecules of interest were applied to the Au electrodes by immersing entire wafers with 15 structures each in beakers containing ethanol based solutions. Wafers were held in these solutions for 24 hours. Before testing, each wafer was removed, cleaned in ethanol, and blown dry with nitrogen. Results for $C_{14}H_{29}$-SH and C_6H_{11}-SH are shown in figures 12 and 13, respectively. The junction resistances for these two 'insulator' type molecules are similar to those measured for nominally clean Au electrodes, ~1 MΩ. This result suggest that either the monolayers did not form as expected, or that the process of dielectrophoretic trapping is too disruptive to the SAM, such that the nanosphere touch the Au electrodes directly. Results

obtained on the last molecular specie analyzed, HS-C_6H_4-SH, suggest that the later explanation, of the balls pushing the molecules apart, is more likely. Since this molecule has a thiol on both ends, it is expected to bond to both the electrodes as well as the nanospheres. This is exactly what is observed when a suspension of Au nanospheres is applied to the electrodes: electrodes become completely covered with spheres. Figure 14 shows the SEM images and I/V characteristics for two junctions formed with electrodes soaked in dithiol benzene. The electrodes shown in 14(a) exhibit characteristically 1 M□ resistance, which is potentially due to the nanosphere 'coating' peeling off, while the junction shown in figure 14 (b) has a very low resistance.

7. Nanogap junctions created using electromigration

In order to circumvent the difficulties associated with bridging electrodes with nanospheres, which potentially disrupt the molecular monolayers, electrode gaps with molecular dimensions are also included in the MONET platform. Molecular dimensions are ~1 nm for 1,4 dithiol benzene, and ~2.5 nm for $C_{14}H_{29}$-SH. To fabricate gaps with these dimensions, we combine EUVL fabrication with electromigration. Figure 15 shows the before and after SEM images of a junction broken by passing a current of ~14 mA. The current vs. time, as well as the I/V plots for this junction are also shown in the same figure. As can be seen, no current is measured above pA noise even at 4 V bias. SEM images of other similarly prepared junctions are shown in figure 16. Interrogation of these junctions after SEM analysis and several days in laboratory ambient showed no change in I/V characteristics. We are currently attempting to place molecules directly into such junctions.

8. Conclusion

We have demonstrated for the first time the use of a bilevel photoresist with EUVL, consisting of PMGI as the bottom layer and Shipley 2D photoresist as the top imaging layer. We have measured the sensitivity of PMGI to EUV radiation and determined appropriate processing conditions for the bilevel photoresist stack. We have shown that metal lift-off with this photoresist is dramatically improved. We have used EUVL and our bilevel photoresist to fabricate an electrode test structure for molecular and nanocrystal characterization. The first molecular systems investigated using the electrode test structure suggest that bridging ~80 nm gaps using Au nanospheres is potentially disruptive to the molecular layers deposited on the electrodes, and thus may yield questionable results. The technique may, however, prove very useful for nanowire and nanocrystal electrical characterization. Finally, we have shown that nanogaps can be formed using electromigration, and that these gaps are stable with time and after SEM inspection. This work was performed at Sandia National Laboratories supported by the U. S. Department of Energy under contract DE-AC04-94AL85000. Sandia is a multiprogram laboratory operated by Sandia Corporation, a Lockheed Martin Company, for the United States Department of Energy.

References

[1] C. P. Collier, E. W. Wong, M. Belohardsky, F. M. Raymo, J. F. Stoddart, R. S. Williams, J. R. Heath, "Electronically configurable molecular-based logic gates", Science **285**, 391 (1999).

[2] J. Chen, M. A. Reed, A. M. Rawlett, J. M. Tour, 'Large on-off ratios and negative differential resistance in a molecular electronic device', Science **286**, 1550 (1999).

[3] E. Lerner, "Big step toward molecular electronics", The Industrial Physicist, December issue, 9 (2002); J. Markoff, "Hewlett takes a step forward in the world of tiny chips" New York Times Section C, page 1, Sep. 10, 2002; also see: http://www.micromagazine.com/archive/02/10/breakout2.html

[4] C. Joachim, "Molecular and intramolecular electronics" Superlattices and Microstructures **28**, 305 (2000).

[5] C. R. Treadway, M. G. Hill, and J. K. Barton, "Charge transport through a molecular π-stack: double helical DNA", Chem. Phys. **281**, 409 (2002).

[6] C. J. Yu et al., 'Electronic detection of single-base mismatches in DNA with ferrocene-modified probes', J. Am. Chem. Soc. **123**, 11155 (2001).

[7] D. A. Tichenor, W. C. Replogle, S. H. Lee, W. P. Ballard, A. H. Leung, G. D. Kubiak, L. E. Klebanoff, S. Graham, J. E. M. Goldsmith, K. L. Jefferson, J. B. Wronosky, T. G. Smith, T. A. Johnson, H. Shields, L. C. Hale, H. N. Chapman, J. S. Taylor, D. W. Sweeny, J. A. Folta, G. E. Sommargren, K. A. Goldberg, P. Naulleau, D. T. Attwood, E. M. Gullikson, Emerging Lithographic Technologies VI, R. L. Engelstad, Editor, Proceedings of SPIE **4688**, 72 (2002).

[8] K. B. Nguyen, G.F. Cardinale, D.A. Tichenor, G. D. Kubiak, K. Berger, A. K. Ray-Chaudhuri, Y. Perras, S. J. Haney, R. Nissen, K. Krenz, R. H. Stulen, H. Fujioka,C. Hu, J. Bokor, D. M. Tennant, L. A. Fetter, J. Vac. Sci. Technol. B 14, 4188 (1996).

[9] S. K. Ghandi, *VLSI Fabrication Principles*, 2nd Ed., John Wiley & Sons, New York, 1994.

[10] R. Williams, *Modern GaAs Processing Methods*, Artech House, USA 1990.

[11] H. Takano, H. Nakano, H. Minami, K. Hosogi, N. Yoshida, K. Sato, Y. Hirose, N. Tsubouchi, J. Vac. Sci. Tech. B **14**, p. 3483, 1996.

[12] See www.microchem.com

[13] J. E. M. Goldsmith, K. W. Berger, D. R. Bozman, G. F. Cardinale, D. R. Folk, C. C. Henderson, D. J. O'Connell, A. K. Ray-Chaudhuri, K. D. Stewart, D. A. Tichenor, H. N. Chapman, R. Gaughan, R. M. Hudyma, C. Montcalm, E. A. Spiller, J. S. Taylor, J. D. Williams, K. A. Goldberg, E. M Gullikson, P. Naulleau, J. L. Cobb, *Emerging Lithographic Technologies III*, Y. Vladimirsky, Editor, Proceedings of SPIE **3676**, 264 (1999).

[14] R. L. Brainard, C. Henderson, J. Cobb, W. Rao, J. F. Mackevich, U. Okoroanyanwu, S. Gunn, J. Chambers, S. Connolly, J. Vac. Sci. Technol. B **17**, 3384 (1999).

[15] A. Bezryadin, C. Dekker, G. Schmidt, Appl. Phys. Lett. 71, 1273 (1997).

[16] P. A. Smith, C. D. Nordquist, T. N. Jackson, T. S. Mayer, B. R. Martin, J. Mbindyo, T. E. Mallouk, Appl. Phys. Lett. 77, 1399 (2000).

[17] I. Amlani, A. M. Rawlett, L. A. Nagahara, and R. K. Tsui, Appl. Phys. Lett. **80**, 2761 (2002).

[18] J. M. Tour and D. K. James, *Handbook of Nanoscience, Engineering, and Technology*, W. A. Goddard III, D. W. Brenner, S. E. Lyshevski, and G. J. Iafrate, editors, CRC Press, 4-1 (2003).

Figures

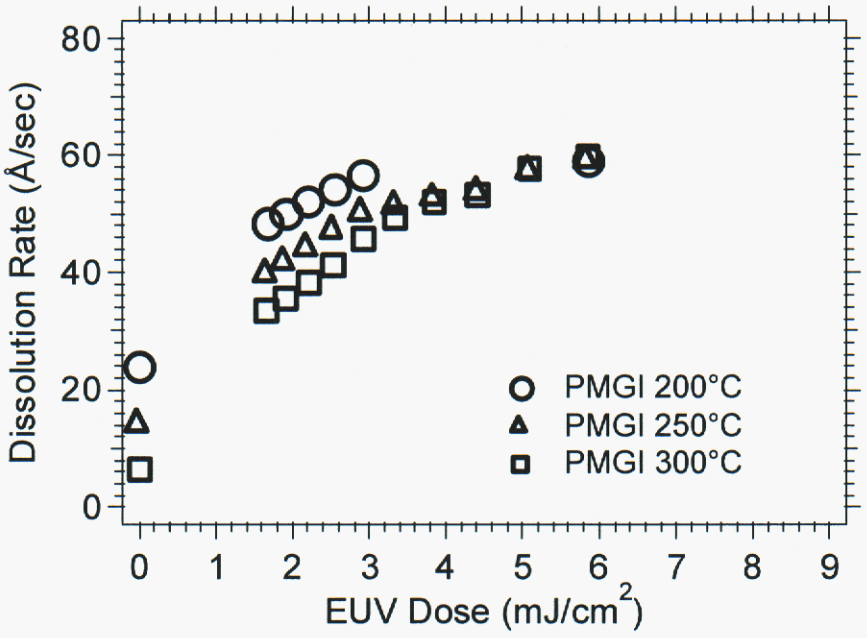

Figure 1. Sensitivity of PMGI photophotoresist to EUV dose, as a function of prebake temperature. Developer: 0.26 N tetramethyl ammonium hydroxide; 5 min prebake time for all temperatures.

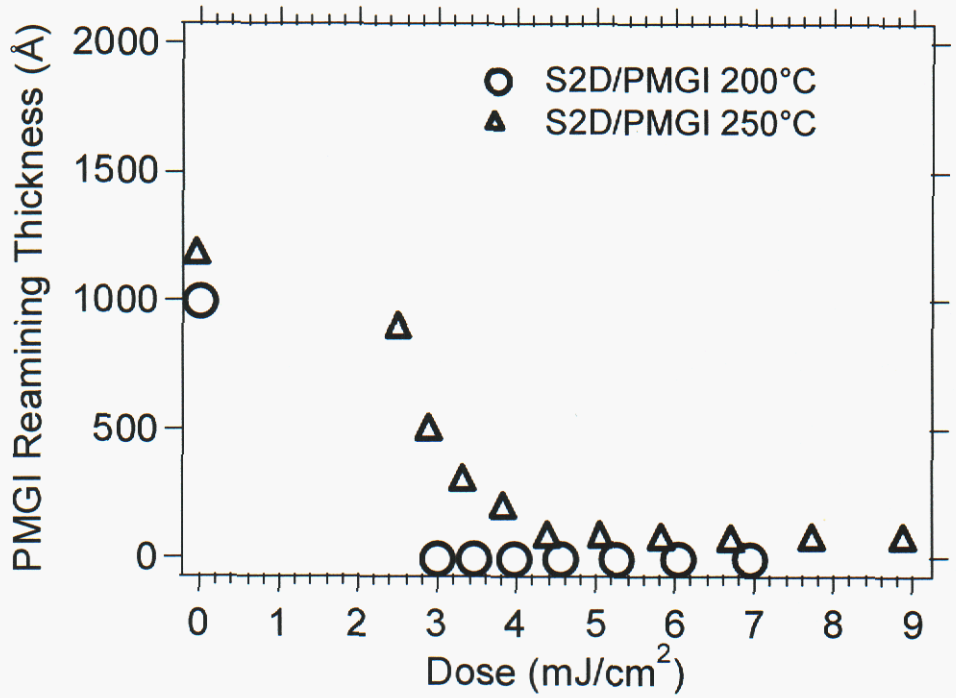

Figure 2. PMGI bottom layer remaining after 60 sec develop time in TMAH as a function of EUV exposure dose of PMGI/S2D bilevel photoresist stacks.

(a)

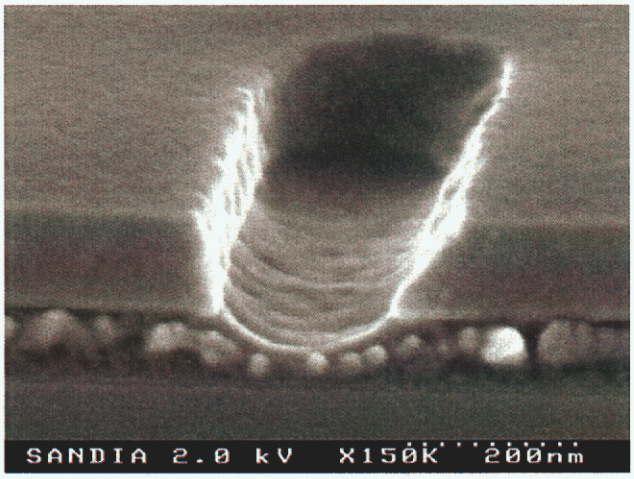

(b)

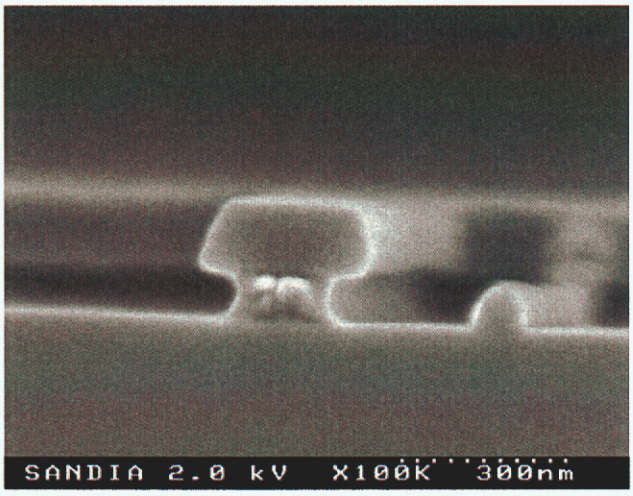

(c)

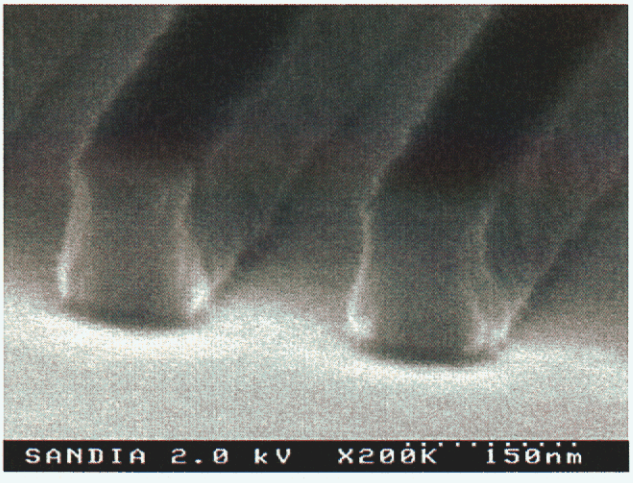

Figure 3. SEM cross-sections of PMGI/S2D photoresist stacks exposed to EUV dose of 3mJ/cmP^{2P}, (a) PMGI pre-bake at 250°C, 60 sec develop in TMAH (b) PMGI pre-bake at 200°C, 60 sec develop in TMAH (c) PMGI nom. thickness 300 Å, pre-bake at 250°C, 45 sec develop in TMAH.

(a)

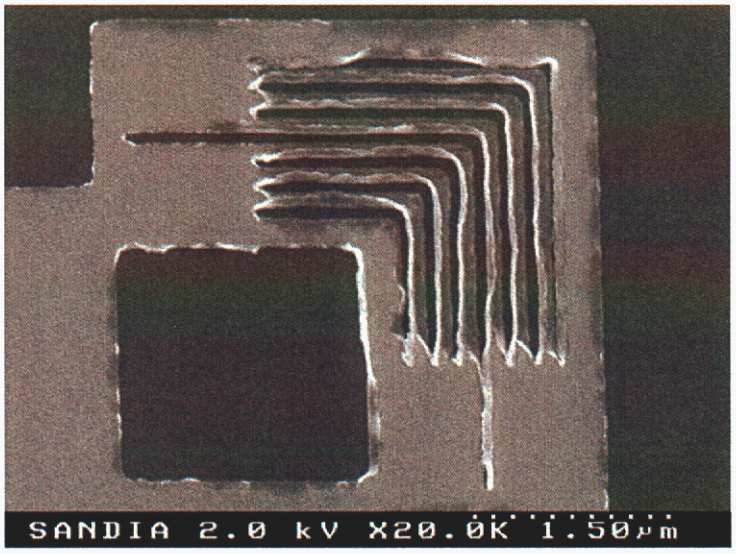

(b)

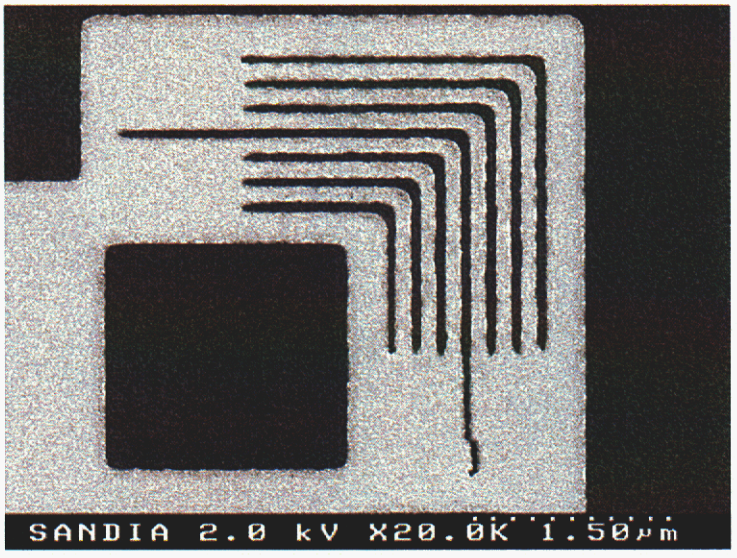

Figure 4. SEM image of 60 nm Au pattern following lift-off in acetone with (a) only 1250 Å of S2D and (b) 300 Å, 250°C PMGI/S2D. No Ti or Cr adhesion layers used in this case.

(a)

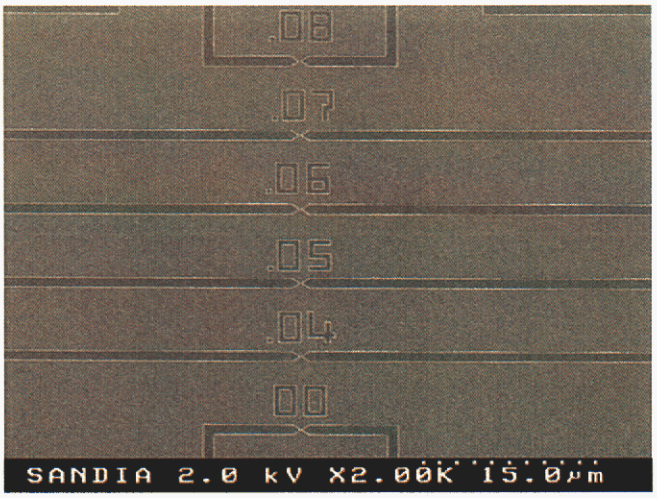

(b)

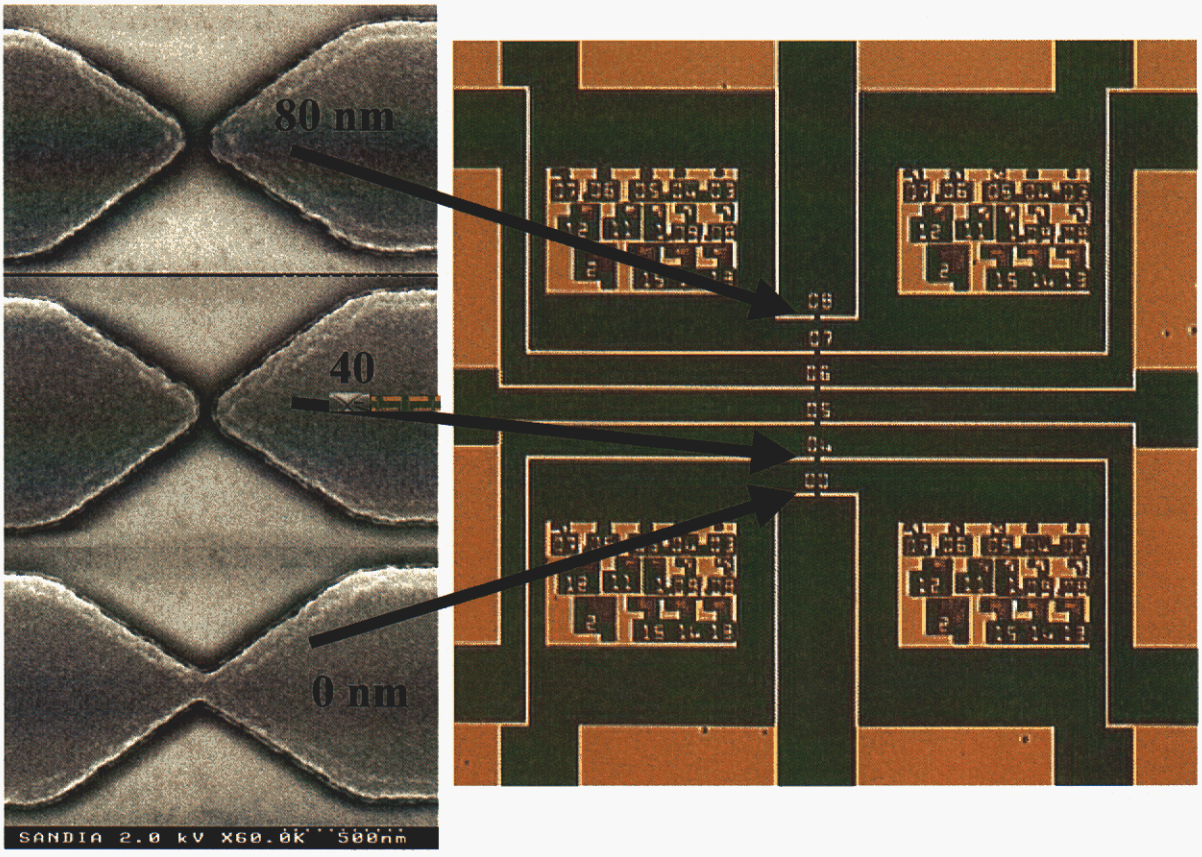

Figure 5. (a) SEM image of EUV MONET mask with patterned TiN absorber layer on Mo/Si multilayer substrate (b) optical image with SEM insets of one MONET structure.

(a) (b) (c)

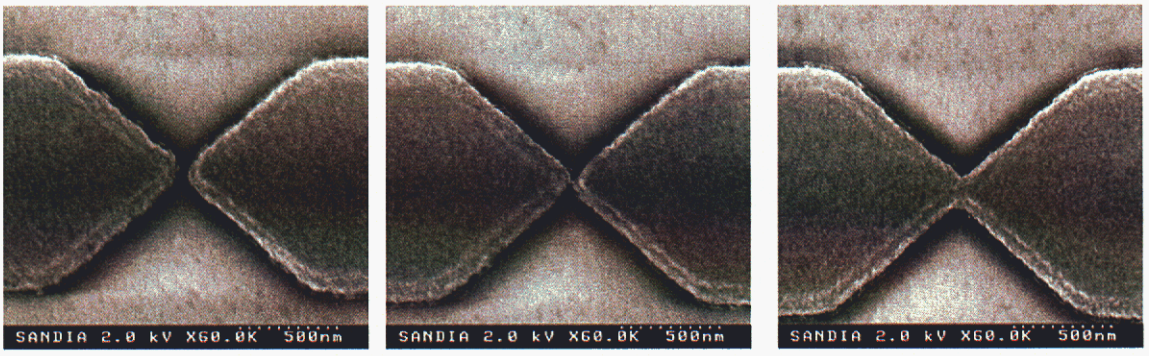

Figure 6. Au electrode structures fabricated on the same $Si/SiOB_{2B}$ substrate using different EUV exposure doses (a) 3.23 mJ/cmP^{2P} (b) 3.71 mJ/cmP^{2P}, (c) 4.26 mJ/cmP^{2}.

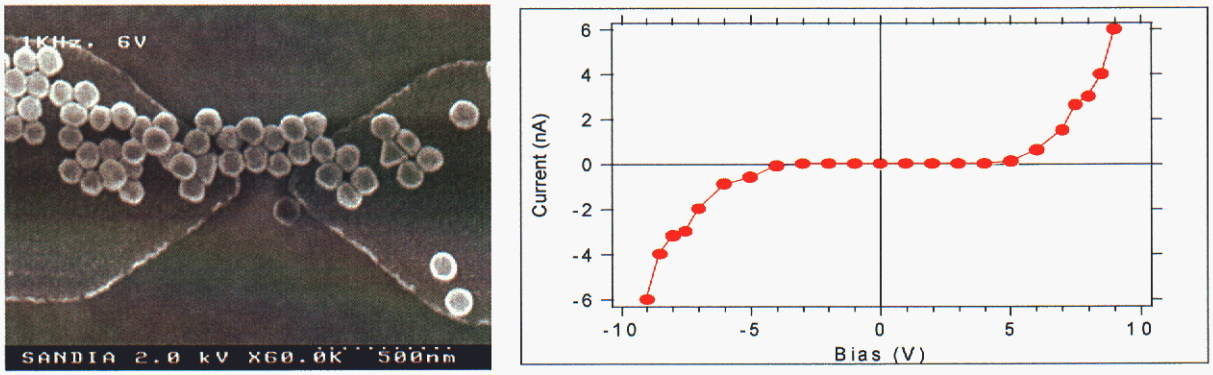

(a) (b)

Figure 7. (a) Au electrode junction bridged by Au nanospheres (b) corresponding I/V characteristic.

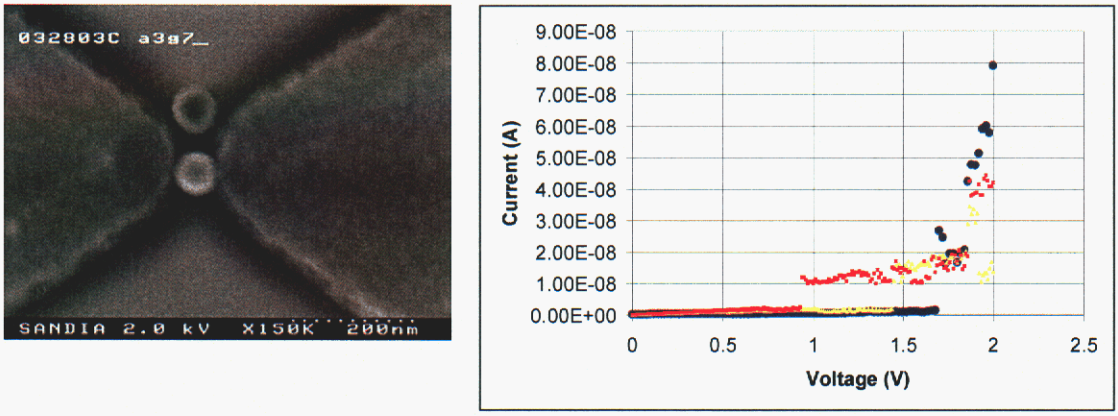

(a) **(b)**

Figure 8. (a) a junction bridged by a single nanosphere and (b) the corresponding I/V profile; the different colors represent successive traces, with the yellow trace taken 24 hours after the blue and pink traces.

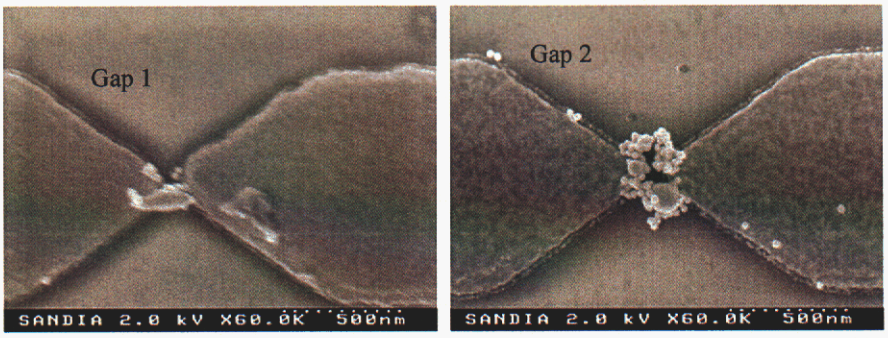

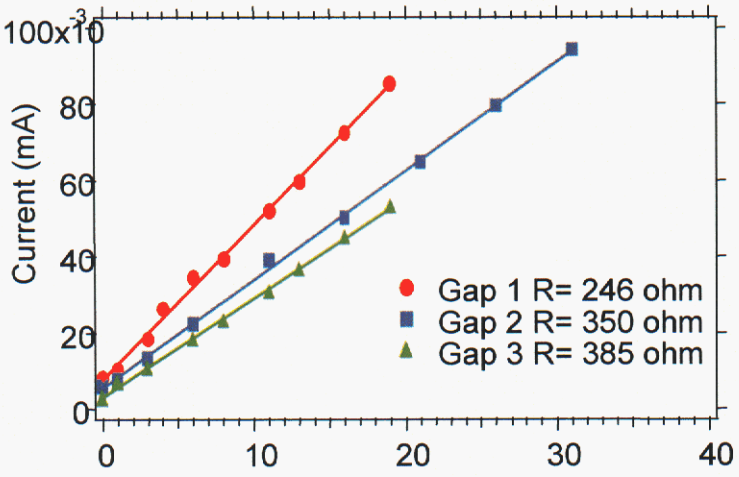

Figure 9. Two junctions bridged by 30 nm nanospheres and showing melting with low resistances.

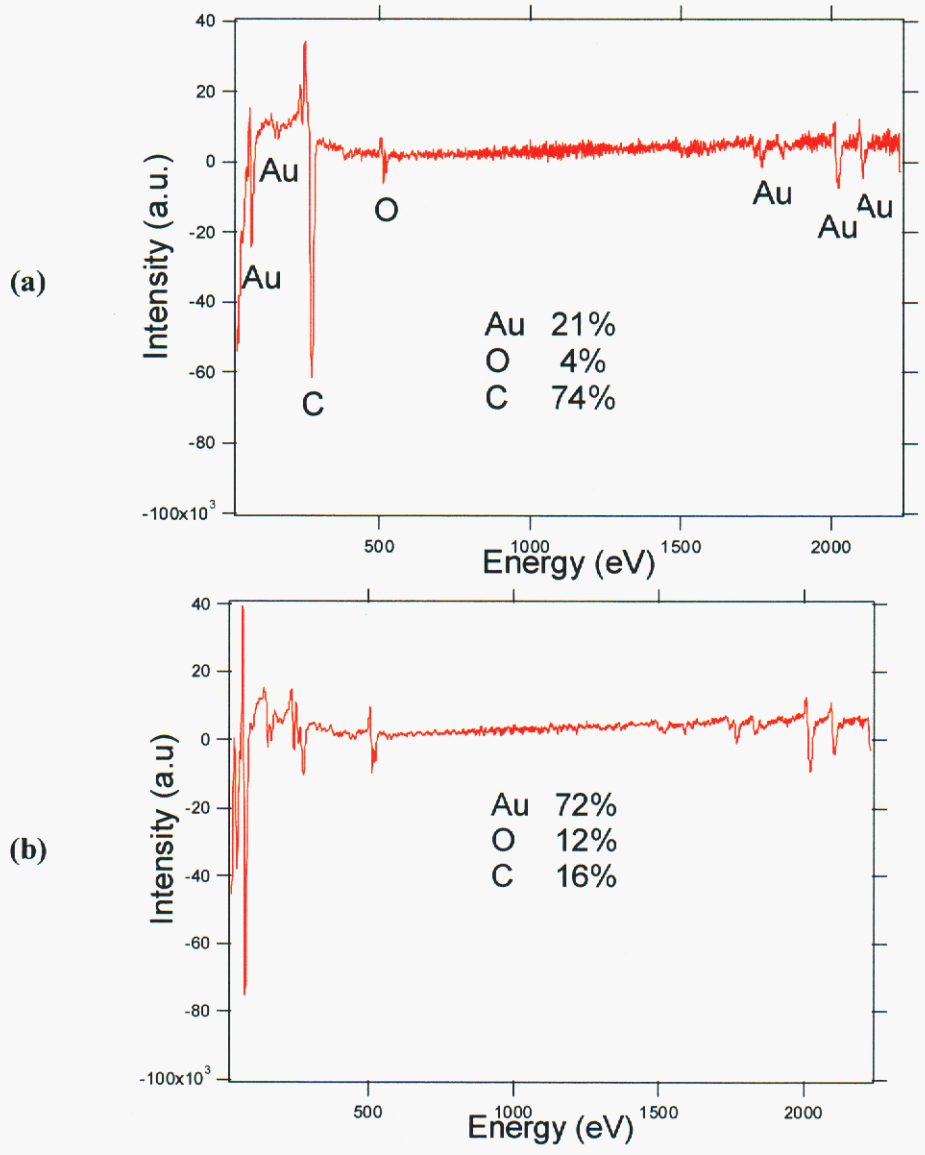

Figure 10. AES spectra of (a) as-fabricated and (b) oxygen plasma cleaned Au electrodes. Spectra were collected near the tip of electrodes.

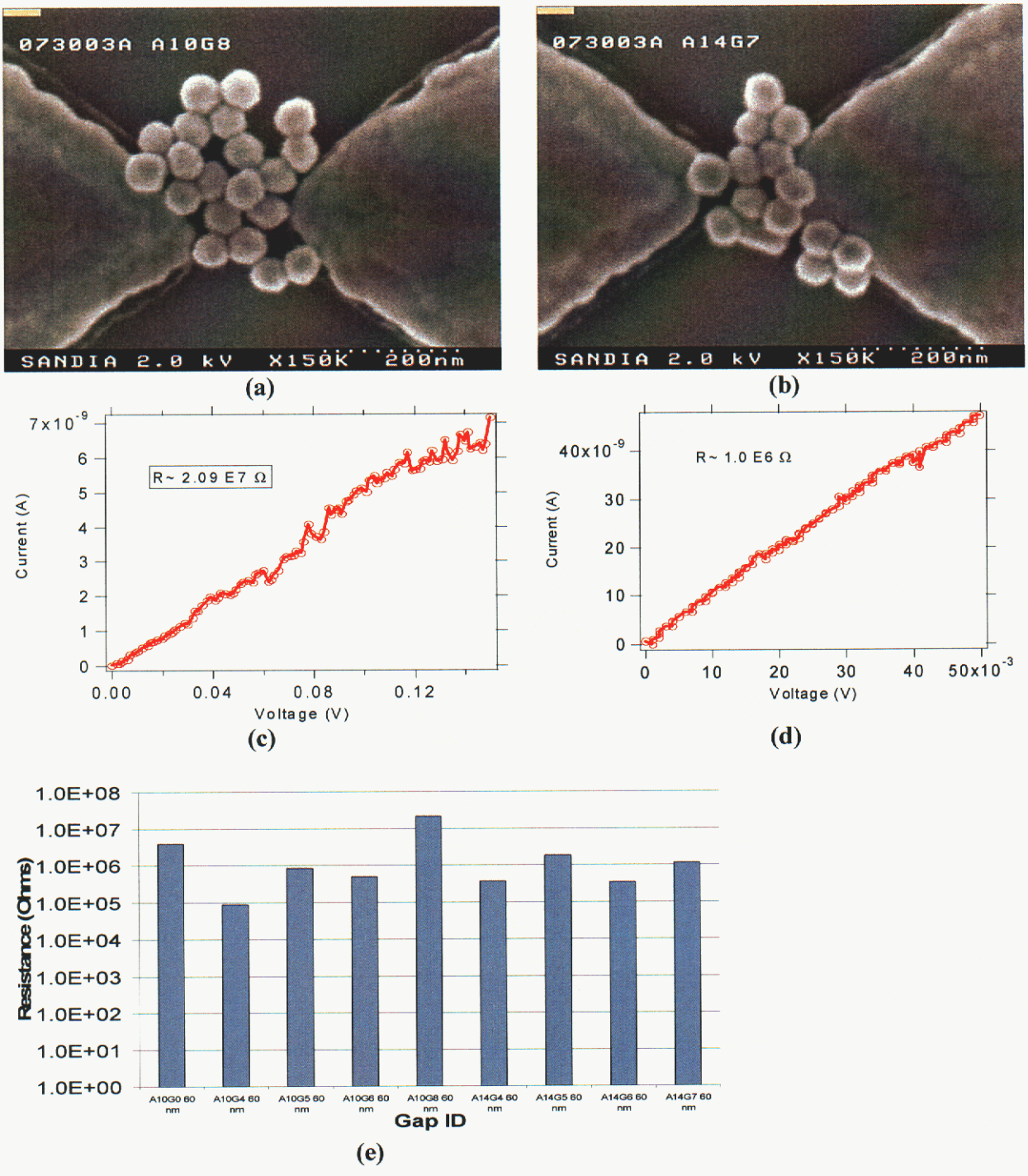

Figure 11. (a), (b) SEM images and (c), (d) corresponding I/V curves for two junctions formed using 60 nm Au spheres on cleaned Au electrodes. (e) a histogram showing junction resistance distribution for similarly formed junctions.

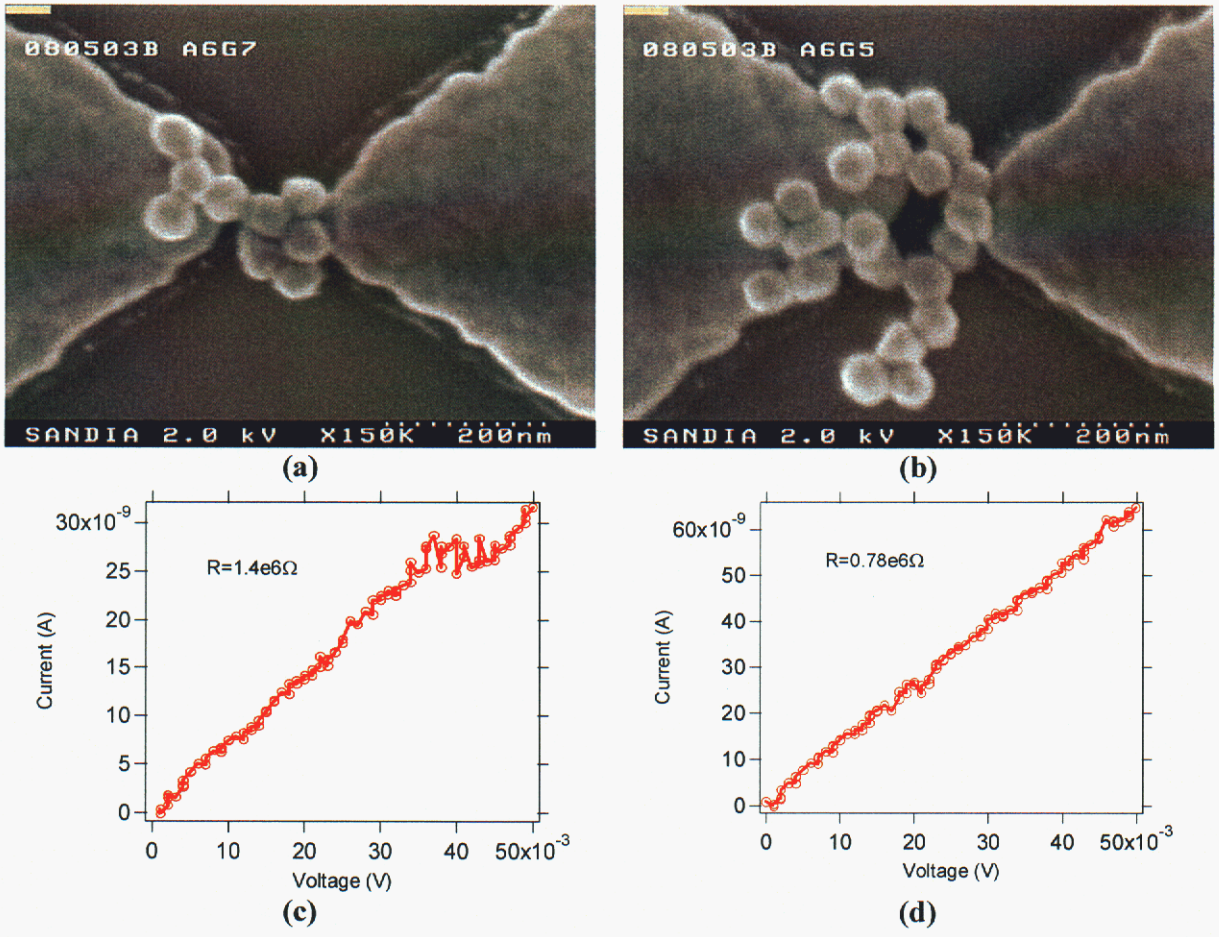

Figure 12. (a), (b) SEM images and (c), (d) corresponding I/V curves for two junctions formed using 60 nm Au spheres on cleaned Au electrodes immersed for 24 hours in a solution of $C_{14}H_{29}$-SH. (e) a histogram showin junction resistance distribution for similarly formed junctions.

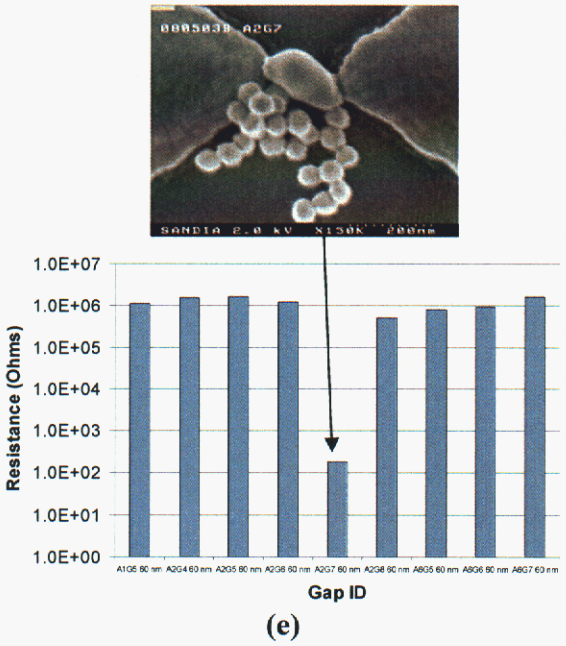

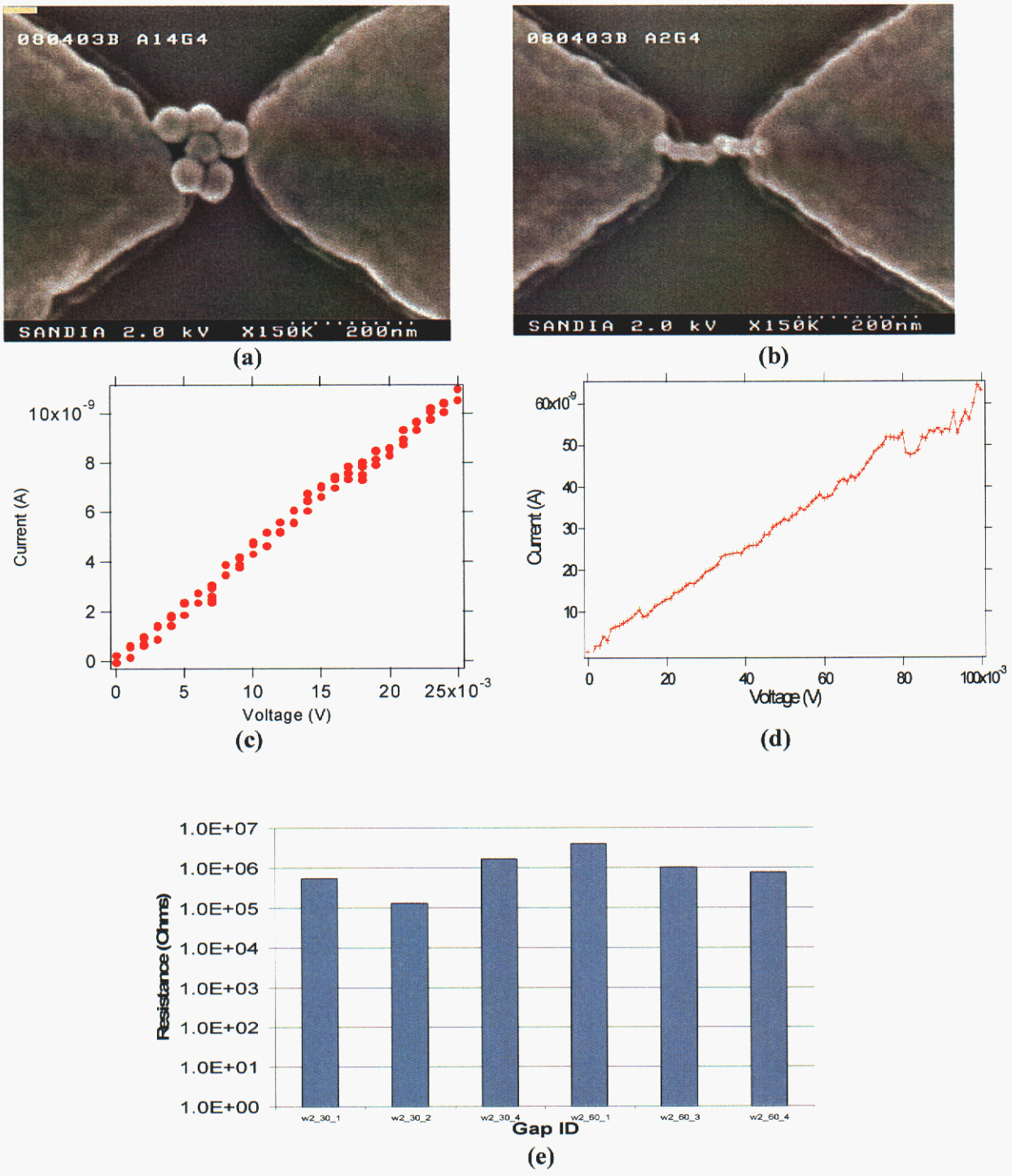

Figure 13. (a), (b) SEM images and (c), (d) corresponding I/V curves for two junctions formed using 60 nm Au spheres on Au electrodes coated with C_6H_{11}-SH. (e) a histogram showing junction resistance distribution for similarly formed junctions.

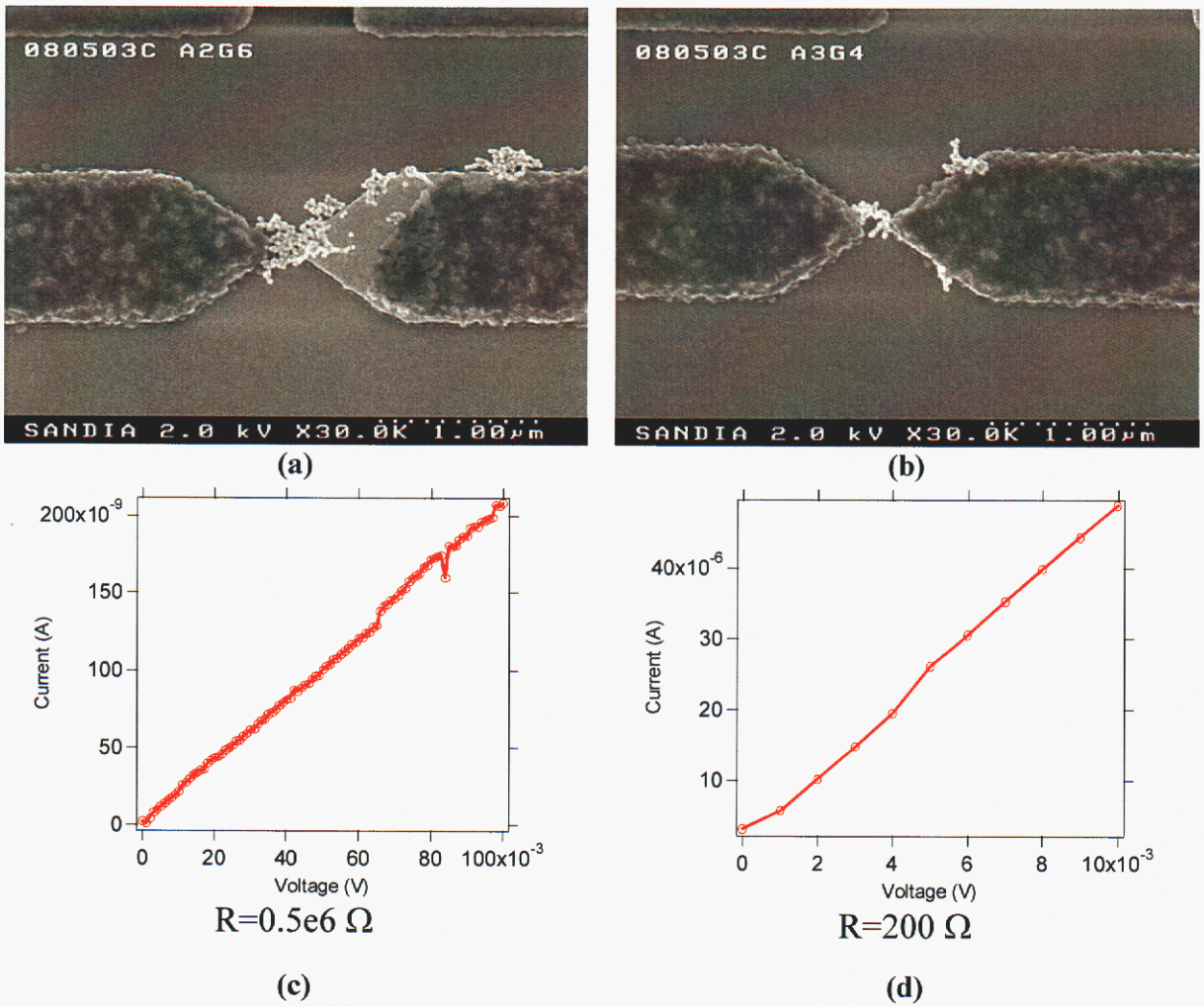

Figure 14. (a), (b) SEM images and (c), (d) corresponding I/V curves for two junctions formed using 30 nm Au spheres on Au electrodes coated with HS-C_6H_4-SH. Note that electrodes are completely covered with nanospheres.

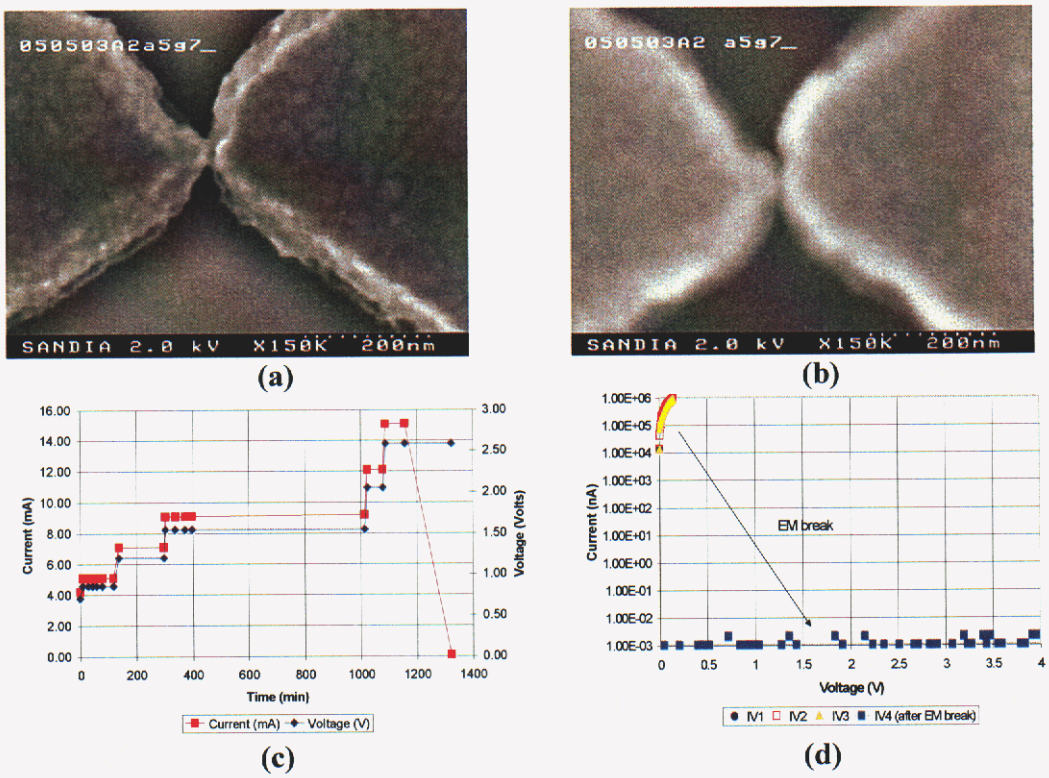

Figure 16. (a), (b), (c), and (d) examples of junctions with nanogaps formed by electromigration. In (c), Ti layer is removed by HF.

DISTRIBUTION:

1	MS0323	D. Chavez, LDRD Office, 1011
1	MS0892	D. R. Wheeler, 1764
1	MS0958	J. A. Emerson, 14172
1	MS1080	D. W. Carr, 1769
1	MS9007	D. R. Henson, 8200
1	MS9036	W. P. Ballard, 8200
10	MS9036	G. F. Cardinale, 8245
1	MS9401	J. M. Goldsmith, 8751
10	MS9401	L. L. Hunter, 8751
10	MS9401	A. A. Talin, 8751
10	MS9403	P. M. Dentinger, 8762
1	MS9403	W. R. Even, 8760
1	MS9403	T. J. Shepodd, 8762
1	MS9404	G. D. Kubiak, 8750
1	MS9405	J. M. Hruby, 8700; Attn:
	MS9042	C. D. Moen, 8752
	MS9042	P. A. Spence, 8774
	MS9161	E-P Chen, 8763
	MS9161	D. L. Medlin, 8761
	MS9402	C. H. Cadden, 8772
	MS9403	J. C. F. Wang, 8773
	MS9404	J. R. Garcia, 8754
	MS9409	W. C. Replogle, 8771
1	MS0899	Technical Library, 9616
3	MS9018	Central Technical Files, 8945-1
1	MS9021	Classification Office, 8511/Technical Library, MS0899, 9616 DOE/OSTI via URL

This page intentionally left blank